# Dynamics of high-angular-momentum velocity-selective coherent population trapping

Chiara Menotti,[1] Peter Horak,[2] Helmut Ritsch,[2] Jörg H. Müller,[1] and Ennio Arimondo[1]
[1]*Unità INFM, Dipartimento di Fisica, Università di Pisa, Piazza Torricelli 2, Pisa 56122, Italy*
[2]*Institut für Theoretische Physik, Universität Innsbruck, Technikerstrasse 25, A-6020 Innsbruck, Austria*
(Received 15 October 1996; revised manuscript received 6 May 1997)

We give a systematic analysis of the extension of the one-dimensional velocity-selective coherent population trapping cooling mechanism to atoms with integer angular momenta $F>1$ using additional light shifts to compensate for the kinetic energy mismatch between the various Zeeman sublevels contributing to the internally decoupled (i.e., dark) state of the atom. Different configurations to achieve the proper light shifts to obtain a very long lifetime of the velocity-selective dark states are discussed and compared. In addition we show that the maximum occupation probability of the resulting quasidark state and its filling time scale strongly depend on the proper choice of detunings to exploit extra precooling mechanisms involving the Zeeman sublevels not contributing to the dark state. We show that additional cooling can also be implemented on the hyperfine repumping transition. This result should prove important for other schemes involving gray states such as, e.g., dark optical lattices and superlattices as well. As a concrete example we consider cesium including all relevant hyperfine levels. [S1050-2947(97)02809-6]

PACS number(s): 32.80.Pj, 42.50.Vk

## I. INTRODUCTION

Light induced cooling of neutral atoms has seen a dramatic decrease in the achievable final temperature during the last decade. Extremely low temperatures (kinetic energies) have been achieved using either velocity-selective coherent population trapping (VSCPT) in He or Rb [1–5] or using Raman induced cooling [6,7] and velocity-selective optical pumping [8]. The VSCPT method is based on optical pumping of atoms into atomic states decoupled from the light fields, which possess a well defined external momentum distribution. Besides yielding very low temperatures this approach has the additional advantage of reducing the atom-atom interaction through photon emission and reabsorption which should prove important in obtaining high phase space densities [9]. So far most of the theoretical and experimental work in this respect has been devoted to $F=1$ to $F=1$ transitions as one can find in metastable He or Rb. In this case the existence of an exactly decoupled velocity-selective atomic state is automatically guaranteed for any nontrivial monochromatic field coupled to this transition [10].

For higher ground-state angular momenta $F>1$ the situation is more complex and no global dark state exists in the general case. However, by introducing suitable $m$-dependent shifts of the Zeeman sublevels the existence of a velocity-dependent dark state can be achieved [11,12]. In this work we study how such shifts can be realized by the help of additional laser fields on other hyperfine transitions providing for the existence of an approximate dark state. We investigate how, in the case of one-dimensional (1D) VSCPT with $\sigma_+$-$\sigma_-$ counterpropagating beams, by a proper choice of the light field configuration and frequencies the effective darkness of this state can be optimized and its filling rate enhanced.

After defining our model and giving a short review on the principles of VSCPT in Sec. II, we investigate various field configurations for which such an approximate dark state exists for angular momentum states $F>1$.

One of the crucial problems of the VSCPT mechanism is its cooling rate and efficiency, which being based on random momentum diffusion strongly decreases in higher dimensions [13]. Hence efficient cooling requires an additional precooling or confinement mechanism [3,14]. One such mechanism by introducing duty cycles between VSCPT and Sisyphus cooling on an $F=1$ to $F=1$ transition was discussed recently by Marte and co-workers [15]. The situation is somewhat changed for higher $F\rightarrow F$ transitions. In this case the system contains a VSCPT-type subsystem ($\Lambda$ or $M$ type) as well as a $W$-type subsystem. Hence, dark-state cooling and polarization gradient cooling can simultaneously occur by a proper choice of the parameters. We investigate this relative cooling efficiency for various detunings and polarizations of the light fields in Sec. III.

As the alkali-metal atoms possess two different hyperfine ground states, it is necessary to introduce some hyperfine repumping. The influence of optical jumps between these two hyperfine levels is often neglected in theoretical treatments of laser cooling. Experimentally this repumping is facilitated by proper sidebands on the cooling lasers or even an extra repumping laser. We show that a proper inclusion of this repumping can lead to important changes in the atomic cooling dynamics. In Sec. IV the effect of various choices for this repumping mechanism on the time scale and efficiency of the dark-state cooling is discussed and compared for various possible repumping schemes.

## II. APPROXIMATE DARK STATES FOR ATOMS WITH ANGULAR MOMENTA $F>1$

It is well known that in a $\Lambda$-type interaction scheme involving two long-lived atomic ground states simultaneously coupled to a single upper state by two different laser fields, one can find certain superpositions of the atomic ground states, which decouple from the light fields and experience no light shift. If the difference in the two laser frequencies just corresponds to the energy separation of the two ground

 

states, this dark state is an eigenstate of the internal atomic dynamics. As this state has no contribution from the upper atomic level it shows no fluorescence, which is why it is called a dark state. As has been shown in Refs. [2,10] such a state can also be an eigenstate of the external atomic degrees of freedom if one considers the case of an $F=1$ to $F=1$ transition coupled to light fields with different wave vectors but equal frequencies. This is related to the fact that besides being internally decoupled from the light fields the external wave functions of all the involved Zeeman sublevels $|\pm 1\rangle$ are given by plane wave states with a momentum equal to a single photon momentum. Hence they are eigenstates of the kinetic energy Hamiltonian with the same eigenvalue $E_{\rm kin}=(\hbar k)^2/(2M)$. Unfortunately this is no longer true if an analogous state including Zeeman sublevels with $m>1$ is constructed. In this case the involved plane wave components connected to the different Zeeman sublevels $|m\rangle$ involve multiples of the photon momentum $\hbar k$. Obviously no global dark state persists if one includes the external atomic motion as the internally decoupled atomic state is no longer an eigenstate of the kinetic part of the Hamiltonian. In the following we will show how this situation can be remedied if one allows for additional light fields, which compensate for this kinetic energy mismatch.

In our one-dimensional model the Hamiltonian in the dipole and rotating wave approximation reads

$$H=\hat{p}^2/2M-\hbar\sum_{j=1,2}\delta_j P_{e_j} + \frac{\hbar}{2}\sum_{j=1,2}\sum_{\sigma}\Omega_j[a_\sigma^j(\hat{x})\hat{A}_\sigma^{j\dagger}+\text{H.c.}], \tag{1}$$

where we consider an atom with a ground state of angular momentum $F_g$ and two excited states $F_{e_j}$. $P_{e_j}$ denotes the projector onto the atomic excited state $|e_j\rangle$, $\delta_j=\omega_{\rm laser}^j-\omega_{ge_j}$ the detuning of the laser frequency relative to the corresponding atomic transition frequency, and $\Omega_j$ the Rabi frequency corresponding to the $j$th atomic transition. $\hat{x}$ and $\hat{p}$ stand for the position and momentum operator, respectively, in the $x$ direction, which is defined by the direction of the incident laser beams. The spatial dependence of the various laser fields is given by the functions $a_\sigma^j(\hat{x})$ (for the laser angular momenta $\sigma=-1,0,1$) and finally the atomic transition operators including the Clebsch-Gordan coefficients are defined as

$$\hat{A}_\sigma^j=\sum_{m_g,m_e}|F_g,m_g\rangle\langle F_{e_j},m_e|\langle F_g,m_g;1\sigma|F_{e_j},m_e\rangle. \tag{2}$$

Let us now briefly review the case of $F=1$. Specializing the Hamiltonian to the case of a single $F=1$ to $F=1$ transition with counterpropagating $\sigma_+$ and $\sigma_-$ fields, it can be easily seen that the state $|\psi_{\rm NC}\rangle=1/\sqrt{2}(|F_g,m_g=-1,p=-\hbar k\rangle+|F_g,m_g=1,p=\hbar k\rangle)$ decouples internally from the laser fields, i.e., $V_{\rm opt}|\psi_{\rm NC}\rangle=0$ where $V_{\rm opt}$ is the potential part of the Hamiltonian (1). Fortunately it is simultaneously an eigenstate of $H_{\rm kin}=\hat{p}^2/2M$. Hence we get an (improper) eigenstate of the total system, which is completely decoupled from the light fields.

Following a similar procedure for the same light field configuration but an $F=2$ to $F=2$ transition, we can also find a noncoupled state which fulfills the first condition $V_{\rm opt}|\psi_{\rm NC}\rangle=0$,

$$|\psi_{\rm NC}\rangle=\sqrt{3/8}|m_g=-2,-2\hbar k\rangle+1/2|m_g=0,0\hbar k\rangle + \sqrt{3/8}|m_g=2,2\hbar k\rangle. \tag{3}$$

However, this state involves plane wave components with different kinetic energy, so that it is no eigenstate of $H_{\rm kin}$. Under the free time evolution given by $H_{\rm kin}$ this state then periodically evolves into the maximally coupled state and back to a noncoupled state. This prevents an accumulation of atoms in this state by conventional dark-state cooling as during the bright periods the atom is optically pumped out of this state. As has been shown recently theoretically by Wu *et al.* [16] and also experimentally by Sander *et al.* [17], using a correlated periodic duty cycle for the VSCPT beams one is able to partly avoid this problem and filter out this state. However, as the cooling can only be effective during the short periods in time, where the state is almost noncoupled, the time scale of this process is fairly slow. In addition other superposition states shifted by even multiples of the photon recoil are also stable against this filtering, so that one does not obtain a pure state at the end.

Here we will use a different approach and try to generate an approximate stationary noncoupled state by compensation of the kinetic energy mismatch between sublevels with different $m$ by some extra external potentials $V_{\rm shift}$. Hence we are looking for a potential $V_{\rm shift}$ so that the internal state, satisfying $V_{\rm opt}|\psi_{\rm NC}\rangle=0$, is also an eigenstate of the remaining Hamiltonian, i.e., we need

$$(H_{\rm kin}+V_{\rm shift})|\psi_{\rm NC}\rangle=E_{\rm NC}|\psi_{\rm NC}\rangle. \tag{4}$$

One possible choice is to use additional far detuned light fields [11,12]. In this case one has to find a transition with the proper Clebsch-Gordan coefficients to ensure the right magnitude and direction of the induced shifts. Moreover, spontaneous emission on this transition, which would destroy the darkness of the prepared state, has to be avoided. Hence one has to use very large detunings on one hand, but on the other hand one has to avoid additional unwanted shifts induced on other transitions. Fortunately the rich angular momentum structure (fine structure and hyperfine structure) of the alkali metal provides several possibilities to achieve this.

Before presenting possible solutions for this problem let us introduce a further simplification of our treatment. Let us assume that the field strengths and detunings are chosen in such a way that the excited states are only weakly populated and can be adiabatically eliminated [18]. Although this assumption might not be strictly fulfilled in some possible VSCPT setups, we do not expect major changes in the obtained results. On the other hand, especially for the case of high $F$ the calculational effort is substantially reduced in this limit. The total Hamiltonian including the compensating light shift fields then reads

$$H_{\rm ad}=\hat{p}^2/2M+\hbar\sum_{j=1,2}U_j V_j(\hat{x}), \tag{5}$$

TABLE I. Optimal values for the light shift of the compensation lasers for different transitions and polarizations. $U_2$ is given in units of $\omega_R$.

| | $F\rightarrow F-1$ | $F\rightarrow F$ | $F\rightarrow F+1$ |
|---|---|---|---|
| $\pi$ light | $U_2=F(2F+1)$ | $U_2=-F(F+1)$ | $U_2=(2F+1)(F+1)$ |
| $\sigma_+$-$\sigma_-$ light | $U_2=-F(2F+1)/2$ | $U_2=F(F+1)/2$ | $U_2=-(2F+1)(F+1)/2$ |

where

$$U_j=s_j\,\frac{\delta_j}{2} \tag{6}$$

is called the optical potential depth and

$$V_j(\hat{x})=\left(\sum_\sigma a_\sigma^j(\hat{x})^\dagger \hat{A}_\sigma^j\right)\left(\sum_\sigma a_\sigma^j(\hat{x})\hat{A}_\sigma^{j\dagger}\right) \tag{7}$$

is the spatial modulation of the optical potential. Furthermore, we can define the optical pumping rate

$$\gamma_j=s_j\,\frac{\Gamma}{2}. \tag{8}$$

We have introduced the saturation parameter $s_j$ on the $j$th transition, defined as

$$s_j=\frac{1}{2}\,\frac{\Omega_j^2}{\delta_j^2+\Gamma^2/4}. \tag{9}$$

Here by the index $j=1$ we always mean a VSCPT-type configuration of counterpropagating $\sigma_+$- and $\sigma_-$-polarized light fields, and by $j=2$ an additional ''compensation'' laser field which will be specified in the following. Note that the compensation fields are assumed to be tuned to a different atomic transition than the VSCPT field, and thus no interference terms between these fields appear in the Hamiltonian (5).

Due to the *coherent* time evolution as described by the kinetic term and the first term of the sum in Eq. (5) the set of magnetic sublevels of the ground state breaks into the decoupled families of states $\mathcal{F}_1(q)$ consisting of the states $|m_g,p=q+m_g\hbar k\rangle$ with $m_g=-F_g,-F_g+2,\ldots,F_g$ and analogous $\mathcal{F}_2(q)$ with $m_g=-F_g+1,-F_g+3,\ldots,F_g-1$. For an arbitrary $F$ to $F-1$ transition there exists one internal noncoupled state in each of the families $\mathcal{F}_1(q)$ and $\mathcal{F}_2(q)$, whereas in an $F$ to $F$ transition only the noncoupled state in $\mathcal{F}_1(q)$ exists. Thus in the families corresponding to family momentum $q=0$ each of the ground-state sublevels building up the noncoupled state has a kinetic energy of $m_g^2\hbar\omega_R$ depending on the magnetic quantum number, where $\omega_R$ is the recoil frequency. Hence, in order to obtain a noncoupled state of $V_1$ which simultaneously is an eigenstate of the full Hamiltonian (5) we have to apply a potential $V_2$ which compensates this kinetic energy mismatch of the different sublevels which form the internal noncoupled state.

Fortunately, due to the properties of the Clebsch-Gordan coefficients used in Eq. (2) the compensation can be achieved in various ways. Because the dark state is decoupled from the VSCPT field, linear in any point of space, in order to produce a light shift the compensating electric field should also be linearly polarized in a direction orthogonal to that of the VSCPT one. We found two different kinds of possible compensation fields.

(i) A light field which is $\pi$ polarized along the quantization axis. In this case every magnetic sublevel $|m\rangle$ is shifted independently by an amount which is, apart from an offset, proportional to $m^2$ due to the properties of the appropriate Clebsch-Gordan coefficients [19].

(ii) A second pair of $\sigma_+$ and $\sigma_-$ light beams counterpropagating along the VSCPT axis, with the $\sigma_+$ beam in phase with the $\sigma_+$ VSCPT one and the $\sigma_-$ beam shifted by a phase of $\pi$ with respect to the $\sigma_-$ VSCPT one [20]. As an example let us consider VSCPT on an $F=2\rightarrow 2$ transition. The dark state fulfilling $V_1|\psi_{\rm NC}\rangle=0$ is given by Eq. (3). It can be worked out from Eqs. (2) and (7) that a $\sigma_+$-$\sigma_-$ compensation field as described here will act on this state as

$$V_2|\psi_{\rm NC}\rangle=\frac{1}{\sqrt{6}}\,|2,2\hbar k\rangle+|0,0\hbar k\rangle+\frac{1}{\sqrt{6}}\,|-2,-2\hbar k\rangle, \tag{10}$$

while the kinetic energy operator applied to this state yields

$$\frac{\hat{p}^2}{2M}\,|\psi_{\rm NC}\rangle=4\hbar\omega_R\sqrt{\frac{3}{8}}\,(|2,2\hbar k\rangle+|-2,-2\hbar k\rangle). \tag{11}$$

Thus if we choose $U_2=3\omega_R$, we find that $H_{\rm ad}|\psi_{\rm NC}\rangle=6\hbar\omega_R|\psi_{\rm NC}\rangle$, i.e., $|\psi_{\rm NC}\rangle$ is an eigenstate of the full Hamiltonian.

It can be shown that both schemes work for compensation transitions of $F$ to $F-1$, $F$, and $F+1$. For all these cases, the value of the optical potential strength $U_2$ required for compensating exactly the kinetic energy difference is given in Table I. Note that in the case of compensation by $\sigma_+$ and $\sigma_-$ light the difference in the laser frequency between the VSCPT and the compensation transition may introduce superlattice effects, as has been recently discussed for an $F=1$ to $F=1$ transition [14,21]. However, in the present work we will suppose that we are dealing with two hyperfine transitions very close in wavelength and the difference in the wave number will be neglected. Let us emphasize again that the compensated dark states are *bright* with respect to the compensation field, which will thus introduce coherent couplings to the excited states. Hence in order to avoid significant optical pumping out of the dark state, the compensation field must be far off resonance. The item of optical pumping will be addressed in the next section.

As an example of the role of the compensating potential, we plot the momentum distribution of the compensated noncoupled (dark) state of an $F=2$ to $F=1$ or $F=2$ transition in Fig. 1. For the $2\rightarrow 1$ transition two distinct dark states exist, which in steady state will both be significantly popu-

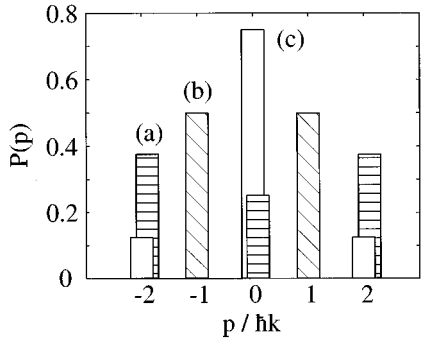


FIG. 1. Momentum distributions for the compensated dark state of (a) a $2\rightarrow 2$ transition and (b), (c) for the two dark states of a $2\rightarrow 1$ transition.

lated. The momentum distribution of these states shows five peaks, the higher one for $p=0$ and the lower ones corresponding to $p=\pm 2\hbar k$. On the other hand, for the $2\rightarrow 2$ transition only one dark state exists: the momentum distribution shows only three peaks distant $2\hbar k$ one from the other and favors the larger momenta $\pm 2\hbar k$.

If the exact compensating potential is applied, $|\psi_{\mathrm{NC}}\rangle$ as defined in Eq. (3) is an eigenstate of the full Hamiltonian (5) and can be denoted a dark state. On the other hand, if the compensation is not exact, the coefficients of the most long-lived eigenstate of the Hamiltonian will be slightly different from those of $|\psi_{\mathrm{NC}}\rangle$ and this state will be called a quasidark state, $|\psi_{\mathrm{QD}}\rangle$.

To demonstrate the effect of the compensation scheme Fig. 2 shows the decay rate of the quasidark state, due to optical pumping cycles on the VSCPT transition. If the optical pumping rate on this transition is $\gamma_1$ [Eq. (8)], this rate is given by $\Gamma_{\mathrm{QD}}=\gamma_1\langle\psi_{\mathrm{QD}}|V_1|\psi_{\mathrm{QD}}\rangle$. Only for exact compensation, i.e., for the dark state, no decay on the VSCPT transition occurs. With increasing laser power of the VSCPT lasers the quasidark state becomes less sensitive to the compensation field, since then the potential part in the Hamiltonian dominates over the kinetic term and the quasidark state approximates more closely the exact internal dark state of $V_1$.

### III. DYNAMICS OF VSCPT COOLING

In this section we will discuss the incoherent dynamics of our system by including spontaneous emission. As mentioned above, this implies a redistribution of the atoms among various momentum states.

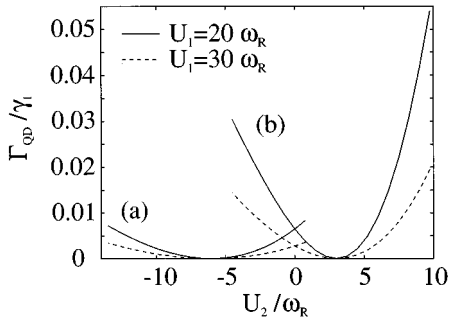


FIG. 2. Decay rate $\Gamma_{\mathrm{QD}}$ of the quasidark state for an $F=2$ to $F=2$ transition as a function of the compensation strength $U_2$. The compensation is achieved by either using (a) $\pi$ or (b) $\sigma_{\pm}$-polarized light.

When spontaneous emission is included, after the adiabatic elimination of the excited states, we obtain a non-Hermitian part in the effective Hamiltonian, which describes the decay of the ground states. The effective Hamiltonian can be written in the following way:

$$h_{\mathrm{eff}}=\hat{p}^2/2M+\hbar\sum_{j=1,2}\left(U_j-\frac{i}{2}\,\gamma_j\right)V_j(\hat{x}). \tag{12}$$

The time evolution of the ground-state density operator including all the internal and external dynamics is then described by the master equation given in the Appendix, Eq. (A14). We calculate the atomic steady state as well as the time evolution using a rate equation approach [22].

To this end we numerically diagonalize the Hermitian part of $h_{\mathrm{eff}}$ [see Eq. (5)] on a spatial grid extending over one or few optical wavelengths. The eigenvectors obtained are denoted as $|n\rangle$, $n=0$, 1, etc. Note that these are eigenstates of the complete *internal plus external* coherent dynamics.

In the secular approximation we calculate the transient and the steady-state populations $\Pi_n$ of the eigenstates $|n\rangle$ neglecting the coherences between them. This approximation is allowed if the spacing between any two different levels is much larger than the width of the eigenstates. This usually corresponds to the situation in which $U_j\gg\gamma_j$. However, for any value of $U_j$ and $\gamma_j$ the fulfillment of this condition should be checked.

The rate equations for the eigenstate populations are

$$\frac{d\Pi_n}{dt}=-\Gamma_n\Pi_n+\sum_m\,\gamma_{n\leftarrow m}\Pi_m\,, \tag{13}$$

where $\Gamma_n$ and $\gamma_{n\leftarrow m}$ are, respectively, the total and partial decay rates and they both contain the optical pumping rates of the different transitions (see the Appendix). For the stationary solution only the ratio between the optical pumping rates of the different transitions is important. A change in the value of the optical pumping rates keeping their ratios constant is equivalent only to a change in the time scale of the temporal evolution.

Because of the symmetry $x\rightarrow x+\lambda$ we restrict the calculation to a box in position space, $x\in[-L,L]$, whose length is an integer multiple of the wavelength with periodic boundary conditions. Naturally this limits our momentum space resolution and the accuracy of the predictions for a final temperature. Nevertheless we can get good estimates for the relative time scales and efficiency of the involved cooling mechanisms and the effect of the compensating light fields. This should provide vital information for possible experimental realizations.

A more accurate calculation would require a full quantum Monte Carlo wave function simulation (QMCWFS) [23], which is, however, a lot more computer time consuming and hence not so suited to compare various configurations over a large range of parameters. Systematic comparisons of both approaches in the case of $F=1$ to $F=1$ have shown a surprisingly strong agreement of the two approaches for a wide range of parameters [23].

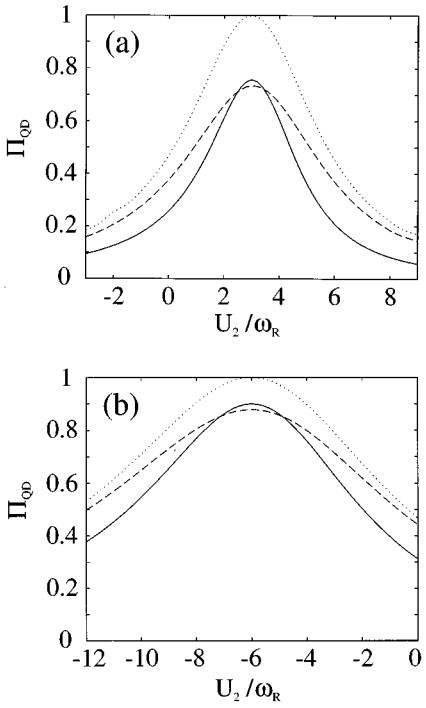


FIG. 3. Dependence of the stationary quasidark-state population on $U_2$ for a $2\rightarrow 2$ transition using (a) $\sigma_{\pm}$- or (b) $\pi$-polarized light for the kinetic energy compensation. The parameters are $U_1=20\omega_R$, $\gamma_2=10^{-3}\gamma_1$ (solid curves), $U_1=30\omega_R$, $\gamma_2=10^{-3}\gamma_1$ (dashed curves), and $U_1=30\omega_R$, $\gamma_2=0$ (dotted curves), respectively.

We have seen in the preceding section how the darkness of the quasidark state depends on the value of the optical potential relative to the light field which produces the kinetic energy compensation. This compensation leads to different values of the steady-state population of this state. We show this dependence in Fig. 3, for the transition $2\rightarrow 2$ and the same values of the parameters used in Fig. 2. In the analysis of Fig. 3 we have supposed that the out of resonance compensating light field, in addition to the light shift compensation, introduces an optical pumping rate $\gamma_2$, small but different from zero, $\gamma_2/\gamma_1=10^{-3}$. Figure 3 shows that even if the decay rate $\Gamma_{QD}$ of the quasidark state is zero for exact compensation, the stationary population is below unity because of the optical pumping rate $\gamma_2$.

Let us now study how the efficiency of the VSCPT process depends on the detuning of the VSCPT transition. For the $1\rightarrow 1$ transition with $\sigma_+$- and $\sigma_-$-polarized light field there are minor changes if the light field is red or blue detuned. Instead for the $2\rightarrow 2$ transition it is possible to observe a cooling force for blue detuning, as has been predicted by semiclassical calculations [24,25]. This can be seen by comparing the momentum distributions for $U_1=30\omega_R$ and $U_1=-30\omega_R$ and interaction time $\gamma_1 t=100$, cf. Fig. 4. For red detuning the atoms are pushed to higher momentum values, while for blue detuning they are pushed to lower momentum values. In Fig. 4, this cooling produces higher wings of the momentum distribution for red detuning and less contrast for the peaks for blue detuning.

Another consequence of this cooling force is observed in the stationary value of the quasidark-state population and in

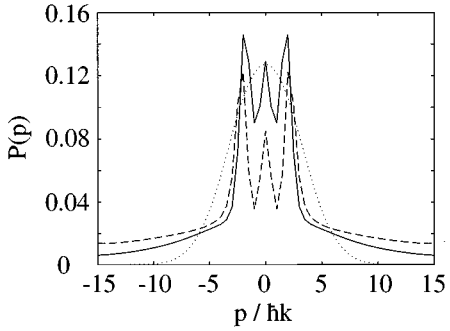


FIG. 4. Transient momentum distribution at time $t=100\gamma_1^{-1}$ for blue detuning ($U_1=30\omega_R$, solid line) and red detuning ($U_1=-30\omega_R$, dashed line) on a $2\rightarrow 2$ transition. The compensation of the dark state was achieved by $\pi$ light with $U_2=-6\omega_R$ and $\gamma_2=0$. The initial distribution (dotted) was chosen as a Gaussian corresponding to a temperature of $k_BT=15\omega_R$.

the filling rate of the quasidark state during the temporal evolution. In Fig. 5 the time evolution is compared for different values of the optical potential depth of the VSCPT field. The following results are obtained for the exact compensation. However, since the main features remain the same even for the case of nonperfect compensation, we will refer more generally to the quasidark state. As before we find for blue detuning faster and more efficient cooling than for the red one. The comparison between different positive values of $U_1$ evidences a better cooling into the dark state for small values, because for large $U_1$, i.e., large Rabi frequency, the internal dark states in the eigenstate families $\mathcal{F}_{1,2}(q\neq 0)$, cf. Sec. II, have long lifetimes [2,15].

In Fig. 5 the time evolution of the quasidark-state population is shown also in the case of some losses of the system. It is well known that VSCPT does not admit a stationary solution, and for very large interaction times there is no more population in the noncoupled state [13]. We will try to approximately investigate this in the following.

In the systems considered until now, the losses of atoms for high velocity are not present. In fact, during the adiabatic elimination of the excited states the commutator with the kinetic energy has been neglected, which is tantamount to neglecting the Doppler shift of the laser frequency [15,26]. Thus the model validity is limited to atom velocities

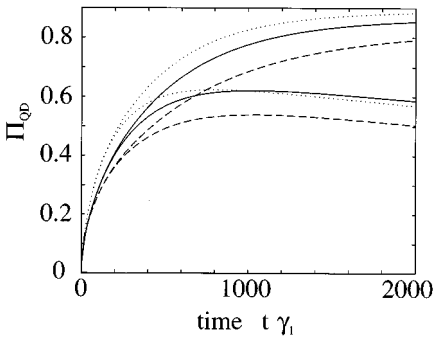


FIG. 5. Temporal evolution of the quasidark-state population with (lower curves) and without losses (upper curves) for $U_1=30\omega_R$ (solid), $-30\omega_R$ (dashed), and $15\omega_R$ (dotted). The compensation is produced by a $\pi$-polarized light field with $U_2=6\omega_R$ and $\gamma_2=10^{-3}\gamma_1$.

$$v < v_D = \sqrt{\hbar\Gamma/M}. \tag{14}$$

Hence only situations with initial *and* final temperatures below the Doppler temperature are described appropriately. However, even in cases violating this condition the relative populations of the lowest few states should be obtained correctly with our model.

The second limitation of our model is due to the finite number of states in the numerical treatment, which introduces a finite maximum velocity for the atom. In an experiment losses out of this group of states, preferentially from fast states, occur as well as feedback from outside into this group. This part of the dynamics cannot be treated in our model.

In order to mimic this situation we introduce an (artificial) cutoff, dividing the numerically obtained states into ''slow'' and ''fast'' ones, and allow for jumps from ''slow'' to ''fast'' states but not the opposite. Due to this neglect of the return of atoms to slow states we overestimate the losses. Thus the real curve will be in between the ''no loss'' and the ''no return'' results.

The main difference between the ''no loss'' and the ''no return'' situations is the following: in the first case the trapped atomic population is always increasing towards the steady-state value; in the second case, it always tends to zero for very large interaction times. It is only in the overidealized situation where the quasidark state is exactly compensated and the optical pumping rate vanishes that the trapped population does not decrease to zero.

However, it should be emphasized that for a large enough cutoff parameter the curves get close to each other for short interaction times. On the other hand, for a reasonable model we must respect the condition (14). Hence if the change of the curve due to the increase of the cutoff is small and the cutoff velocity still obeys Eq. (14), we should be close to the experimental case.

Numerically the ''no return'' model corresponds to solving the rate equation only for the slow states, keeping the same value for the total decay rate $\Gamma_n$ as in Eq. (13), but summing the decay from the other eigenstates only over those states belonging to the subset of slow states. Thus we neglect the contribution of decays from fast to slow states,

$$\frac{d\Pi_n}{dt} = -\Gamma_n \Pi_n + \sum_{m_{\text{slow}}} \gamma_{n\leftarrow m}\Pi_m . \tag{15}$$

As a consequence of the modification in Eq. (15) the quasidark-state population increases until a certain quasiequilibrium is reached, but then starts to fall off due to the nonexact darkness of this state and the loss of atoms with large velocities (Fig. 5). Asymptotically the quasidark-state population tends to zero.

## IV. PRECOOLING VIA REPUMPING FROM THE SECOND HYPERFINE LEVEL

An important point, left out so far, as in most previous treatments of VSCPT cooling, is related to the hyperfine splitting of the alkali-metal ground states. Most of the optical transitions starting from one hyperfine ground state are not closed and the atoms are optically pumped into the other hyperfine state. This applies to the $F$ to $F$ transitions for which the branching ratio to the ground states with different $F$ values has a comparable order of magnitude. In effect all the cooling experiments in alkali-metal atoms require the presence of a repumping laser bringing the atoms back in interaction with the cooling laser. Although being definitely experimentally relevant, this loss-repumping process is often left out or just accounted for by a simple global repumping rate. We have investigated this repumping process in detail. We have found that a suitable choice of the repumping fields not only minimizes the loss effects but also introduces an additional precooling mechanism which enhances the efficiency of the VSCPT process itself. Such an operation of the repumping as an additional precooling process has been applied for the VSCPT experiment in Rb by Esslinger *et al.* [3].

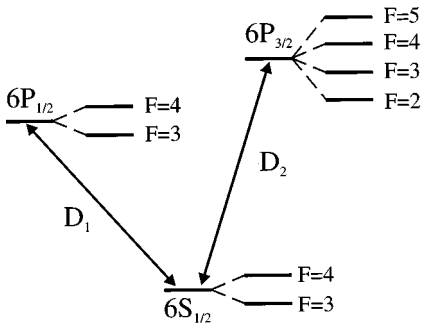


FIG. 6. Level scheme of Cs. The configuration discussed in Sec. IV as an example consists of a VSCPT light field on the $F=3$ to 3 transition of the $D_2$ line, a compensating $\pi$-polarized light field on $3\rightarrow 3$ of the $D_1$ line, and a repumping light field on $4\rightarrow 4$ of the $D_2$ line.

As an example we discuss the level scheme of cesium, see Fig. 6, with two ground-state ($6\,^2S_{1/2}$) levels with $F=3$ and $F=4$ hyperfine quantum numbers. As excited levels there are two different hyperfine multiplets ($6\,^2P_{1/2}$ and $6\,^2P_{3/2}$). Due to the very large splitting between the $F=3$ and the $F=4$ levels in the $6\,^2P_{1/2}$ multiplet this transition offers the possibility of large laser detunings without significant simultaneous excitation of more than one hyperfine level. Hence a laser at this line is best suited for the compensation of the kinetic energy mismatch of the noncoupled state as discussed in the previous sections. Note, however, that for a detailed comparison of the theory with an experiment it is often not possible to neglect the excitation of the second hyperfine level. But since such an off-resonant coupling does not introduce new physical phenomena this coupling will be neglected here.

In the following, we report the results obtained with a light-shift compensation by $\pi$-polarized light on a $F=3\rightarrow F=3$ transition, VSCPT performed on the second $F=3\rightarrow F=3$ transition, and repumping on $F=4\rightarrow F=4$. The light fields for the VSCPT are counterpropagating $\sigma_+$- and $\sigma_-$-polarized laser beams, while for the repumping laser it is possible to choose other configurations. The optical potentials (optical pumping rates) on the various transitions are denoted by $U_j$ ($\gamma_j$), $j=1,\ldots,3$, where $j=1$ refers to the VSCPT transition, $j=2$ to the compensation transition, and $j=3$ to the repumping transition.

For the results reported in Fig. 7 the repumping consists

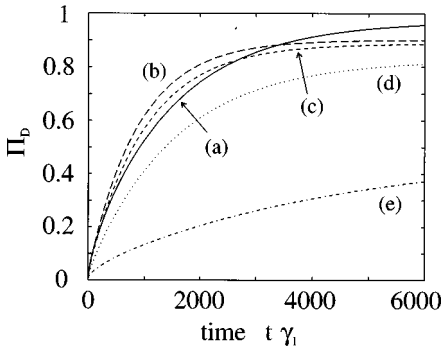


FIG. 7. Dark-state population vs interaction time for VSCPT on the $F=3\rightarrow F=3$ transition for Cs atoms. For all curves we have chosen $U_1=100\omega_R$, $\gamma_2=10^{-3}\gamma_1$, and a Gaussian initial momentum distribution of $k_BT=15\omega_R$. Curve (a) includes only the VSCPT and the light-shift compensation fields, i.e., a model without second ground-state level. The other curves hold for the full model with repumping parameters (b) $U_3=60\omega_R$, $\gamma_3=10\gamma_1$, (c) $U_3=0$, $\gamma_3=10\gamma_1$, (d) $U_3=0$, $\gamma_3=\gamma_1$, (e) $U_3=0$, $\gamma_3=0.1\gamma_1$.

of two counterpropagating light fields of perpendicular linear polarization (lin$\perp$lin). In the presence of a perfect light-shift compensation, the time evolution of the dark-state population is compared for different repumping parameters [curves (b)–(e)] and also for the case where the decay towards the second ground-state level is artificially suppressed [curve (a)]. As expected, the final occupation probability of the dark state is lower when the presence of the second hyperfine level is correctly taken into account. However, by a clever choice for the parameters of the repumping laser, it is possible to achieve a very large filling rate of the dark state, at least for the initial times. So for a finite cooling time the existence of the second hyperfine level can even lead to an improved cooling. On the other hand, an improper choice of the repumping parameters can strongly diminish the cooling efficiency. The comparison between curves (b) and (c) in Fig. 7 shows that for a blue detuned repumping laser the cooling efficiency is larger than for a resonant setup, where no cooling by the repumping laser is present. In effect the analysis of the preceding section has shown that for a blue detuning there exists a cooling force on an $F\rightarrow F$ transition. We have found that for red detuning the force pushes the atoms to higher momentum values and thus decreases the efficiency.

The comparison between curves (c), (d), and (e) evidences the role of different optical pumping rates $\gamma_3$ for the case of a repumping transition without light shift ($U_3=0$). The cooling efficiency increases for growing optical pumping rates on the repumping transition. This is due to the faster repumping of the atom into the VSCPT subsystem and thus a shorter storage time in the second hyperfine ground-state level.

## V. CONCLUSIONS

We have demonstrated that by help of extra light fields continuous 1D VSCPT cooling with $\sigma_+$-$\sigma_-$ polarized counterpropagating beams can be extended to transitions with integer total angular momentum larger than one, so that it can also be used for alkali-metal atoms with nuclear spin $I>3/2$. In contrast to the case of an $F=1$ to $F=1$ transition the detunings and intensities of the involved fields have to be chosen more carefully in order to get a short enough cooling time. This is especially true to avoid unwanted off-resonant couplings by additional hyperfine levels and heating due to optical pumping between the two ground-state hyperfine levels. Let us mention here that a 2D or 3D generalization of this scheme is not obvious, as the polarization of the compensation wave vector has to be orthogonal to the cooling light field at any spatial point. Even if one could find such a geometry, an experimental realization seems rather tedious in higher dimensions. On the other hand, a 1D VSCPT cooling could be a very useful source for an atomic interferometer setup, generating most occupation in the extreme states with largest momentum, whence creating coherent beams with two mean component waves with a splitting of several photon momenta (e.g., $8\hbar k$ for $F=4$). This scheme, eventually coupled to coherent adiabatic passage into a single momentum state, generates a source with a very large brightness.

## ACKNOWLEDGMENTS

We thank G. Morigi and H. Stecher for stimulating discussions and T. Pellizzari for computational support. This work was supported by the Österreichischer Fonds zur Förderung der wissenschaftlichen Forschung under Project No. S6506-PHY and by the European TMR Network (ERB FMRX CT96 0002). J.H.M. gratefully acknowledges the European Community for financial support.

## APPENDIX A: FORMULAS FOR GENERAL ATOM-FIELD CONFIGURATIONS

We will show in this appendix the outlines of the calculations which lead to the master equation for the reduced atomic density operator, obtained after the adiabatic elimination of the excited states. In the following we consider the general case of more than one ground hyperfine level and laser field with only one restriction: two different laser fields cannot couple two different hyperfine levels with the same excited level, in order to avoid the creation of coherences between different ground hyperfine levels.

Let us give first the definitions we used for the electric field and hence for the interaction Hamiltonian. For each laser field the positive frequency part of the electric field is defined as

$$\vec{E}^{(+)}=\frac{1}{2}\sum_{\sigma}\vec{\epsilon}_{\sigma}\mathcal{E}, \tag{A1}$$

where $\vec{\epsilon}_{\sigma}$ include the spatial dependence of the laser field

$$\vec{\epsilon}_{\sigma}=a_{\sigma}(\hat{x})\vec{\sigma}, \tag{A2}$$

with

$$\vec{\sigma}_{\pm}=\mp\frac{\vec{\epsilon}_y\pm i\vec{\epsilon}_z}{\sqrt{2}},$$

$$\vec{\sigma}_{\pi}=\vec{\epsilon}_x. \tag{A3}$$

For each transition $j$, which couples the ground states with total angular momentum quantum number $F_g$ to the excited one with total angular momentum $F_e$, we write the atom-laser interaction Hamiltonian in the dipole approximation as

$$\hat{H}_{AL}^{(j)}(\hat{x}) = \frac{\mathcal{E}}{2} \sum_{\sigma} \sum_{m_g, m_e} a_{\sigma}^{(j)}(\hat{x}) \times \langle F_e, m_e | \vec{d} \cdot \vec{\sigma} | F_g, m_g \rangle | F_e, m_e \rangle \langle F_g, m_g | . \tag{A4}$$

Considering all the quantum numbers for each atomic state $|n,[I,(S,L_g),J_g],F_g,m_g\rangle$, we can write the dipole matrix element as (see, e.g., [27])

$$\langle n,[I,(S,L_e),J_e],F_e,m_e|\vec{d}\cdot\vec{\sigma}|n,[I,(S,L_g),J_g],F_g,m_g\rangle = \langle n,L_e\|\vec{d}\cdot\vec{\sigma}\|n,L_g\rangle \frac{1}{\sqrt{2F_e+1}} \langle F_g,m_g;1,\sigma|F_e,m_e\rangle \times \mathcal{R}(SL_gJ_g,SL_eJ_e)\mathcal{R}(IJ_gF_g,IJ_eF_e) \tag{A5}$$

where the factors $\mathcal{R}$ are defined in terms of the $6j$ symbols as

$$\mathcal{R}(IJ_gF_g,IJ_eF_e) = \sqrt{(2F_g+1)(2F_e+1)} \begin{Bmatrix} I & F_e & J_e \\ 1 & J_g & F_g \end{Bmatrix}. \tag{A6}$$

It is possible to define an atomic raising operator, which includes the line strength for different transitions in order to use it in the Hamiltonian,

$$\hat{A}_{\sigma}^{\dagger(F_eF_g)} = \sum_{m_e,m_g} \langle F_e,m_e|1,\sigma;F_g,m_g\rangle \sqrt{2J_e+1}\sqrt{2F_g+1} \times \begin{Bmatrix} I & F_e & J_e \\ 1 & J_g & F_g \end{Bmatrix} |F_e,m_e\rangle\langle F_g,m_g|. \tag{A7}$$

For the transition from the state $|n,[I,(S,L_e),J_e],F_e,m_e\rangle$ to the state $|n,[I,(S,L_g),J_g],F_g,m_g\rangle$ the branching ratio in respect to the decay over all the ground-state levels is

$$(2J_e+1)(2F_g+1)\langle F_e,m_e|1,\sigma;F_g,m_g\rangle^2 \begin{Bmatrix} I & F_e & J_e \\ 1 & J_g & F_g \end{Bmatrix}^2,$$

with the normalization condition

$$\sum_{F_g} \sum_{m_g} (2J_e+1)(2F_g+1)\langle F_e,m_e|1,\sigma;F_g,m_g\rangle^2 \times \begin{Bmatrix} I & F_e & J_e \\ 1 & J_g & F_g \end{Bmatrix}^2 = 1. \tag{A8}$$

We can define the Rabi frequency in a way that it only depends on the quantum numbers $n,S,L,J$ and not on the quantum numbers $F$ and $m$: this is possible since the line strength and the Clebsch-Gordan coefficients are included in the definition of the raising operators,

$$\Omega_{\sigma}^{(j)}(\hat{x}) = -\frac{\mathcal{E}}{\hbar} \frac{\langle n,L_e\|\vec{d}\cdot\vec{\sigma}\|n,L_g\rangle \mathcal{R}(SL_gJ_g,SL_eJ_e)}{\sqrt{2J_e+1}} a_{\sigma}^{(j)}(\hat{x}) = \Omega_j a_{\sigma}^{(j)}(\hat{x}). \tag{A9}$$

Using the atomic raising operators and the Rabi frequency as defined before, the atom-laser Hamiltonian can be rewritten as

$$\hat{H}_{AL}^{(j)}(\hat{x}) = \hat{H}_{AL}^{(+)(j)}(\hat{x}) + \text{H.c.}, \tag{A10}$$

where $\hat{H}_{AL}^{(+)(n)}(\hat{x})$ is the positive frequency part which includes the Rabi frequency and the raising operator,

$$\hat{H}_{AL}^{(+)(j)}(\hat{x}) = \frac{1}{2} \sum_{\sigma} \hbar \Omega_{\sigma}^{(j)}(\hat{x}) \hat{A}_{\sigma}^{\dagger(F_eF_g)}. \tag{A11}$$

Summing over the ground-state levels, we can construct another raising operator which only depends on the excited level

$$\hat{A}_{\sigma}^{\dagger(F_e)} = \sum_{F_g} \hat{A}_{\sigma}^{\dagger(F_eF_g)}. \tag{A12}$$

The operator is important because the projection operator onto the excited states with total angular momentum quantum number $F_e$ has the following form:

$$P_{F_e} = \sum_{\sigma} \hat{A}_{\sigma}^{\dagger(F_e)} \hat{A}_{\sigma}^{(F_e)}.$$

We define the jump operator which describes the entire possible process consisting of a coherent transition $F_g \rightarrow F_e$ (the $j$th atomic transition) followed by a spontaneous emission decay into any of the hyperfine ground states.

$$\hat{B}_{\sigma}^{(j)}(\hat{x}) = \frac{2}{\hbar} \hat{A}_{\sigma}^{(F_e)} \hat{H}_{AL}^{(+)(j)}(\hat{x}). \tag{A13}$$

Performing the adiabatic elimination of the excited states in the equation for the total density matrix, we obtain the master equation for the reduced atomic density operator

$$\dot{\rho}_{gg} = \frac{1}{i\hbar} [h_{\text{eff}}\rho_{gg} - \rho_{gg}h_{\text{eff}}^{\dagger}] + \hbar \sum_j \gamma_j \sum_{\sigma=0,\pm1} \int_{-k}^{+k} \frac{du}{k} N_{\sigma}\left(\frac{u}{k}\right) \times [e^{-iu\hat{x}} \hat{B}_{\sigma}^{(j)}] \rho_{gg} [\hat{B}_{\sigma}^{(j)\dagger} e^{iu\hat{x}}], \tag{A14}$$

where $N_{\sigma}(q)$ defines the angular distribution of the spontaneously emitted photons, $N_{\sigma}(q) = 3(1+q^2)/8$ for circular and $N_{\sigma}(q) = 3(1-q^2)/4$ for linear polarization. The effective Hamiltonian $h_{\text{eff}}$ is

$$h_{\rm eff}=\hat{H}_{\rm kin}+\hbar\sum_j\left(U_j-\frac{i}{2}\gamma_j\right)\sum_\sigma \hat{B}_\sigma^{(j)\dagger}(\hat{x})\hat{B}_\sigma^{(j)}(\hat{x})$$

$$=\hat{H}_{\rm kin}+\hbar\sum_j\left(U_j-\frac{i}{2}\gamma_j\right)V_{(j)}(\hat{x}), \tag{A15}$$

with the optical potentials defined as

$$V_{(j)}=\sum_{\sigma=0,\pm1}\hat{B}_\sigma^{(j)\dagger}(\hat{x})\hat{B}_\sigma^{(j)}(\hat{x}), \tag{A16}$$

which is equivalent to Eq. (7) and where the other quantities are defined in the text [see Eqs. (6), (8), (9)].

Neglecting the coherences between the eigenstates of the Hermitian part of $h_{\rm eff}$, Eq. (13) is derived from Eq. (A14).

The explicit expression for the partial decay rates from the $m$th to the $n$th eigenstate is

$$\gamma_{n\leftarrow m}=\sum_j\gamma_j\int_{-k}^{+k}\frac{du}{k}\sum_{\sigma=0\pm1}N_\sigma\left(\frac{u}{k}\right)|\langle n|e^{-iu\hat{x}}\hat{B}_\sigma^{(j)}(\hat{x})|m\rangle|^2, \tag{A17}$$

and a similar definition for $\gamma_{m\leftarrow n}$.

The total decay rate of the $n$th eigenstate can be obtained by summing the partial decay rates to all the eigenstates:

$$\Gamma_n=\sum_m\gamma_{m\leftarrow n}=\sum_j\gamma_j\langle n|V_j|n\rangle, \tag{A18}$$

where the second equality is verified applying the definition of Eq. (A17).


[1] A. Aspect, E. Arimondo, R. Kaiser, N. Vansteenkiste, and C. Cohen-Tannoudji, Phys. Rev. Lett. **61**, 826 (1988).

[2] J. Lawall, S. Kulin, S. Saubamea, N. Bigelow, M. Leduc, and C. Cohen-Tannoudji, Phys. Rev. Lett. **75**, 4194 (1995).

[3] T. Esslinger, F. Sander, M. Weidemüller, A. Hemmerich, T. W. Hänsch, Phys. Rev. Lett. **76**, 2432 (1996).

[4] D. Boiron, A. Michaud, P. Lemonde, Y. Castin, C. Salomon, S. Weyers, K. Szymaniec, L. Cognet, and A. Clairon, Phys. Rev. A **53**, R3734 (1996).

[5] T. Esslinger, F. Sander, A. Hemmerich, T. W. Hänsch, H. Ritsch, and M. Weidemüller, Opt. Lett. **21**, 991 (1996).

[6] M. Kasevich and S. Chu, Phys. Rev. Lett. **67**, 181 (1991); N. Davidson, H. Lee, M. Kasevich, and S. Chu, *ibid.* **72**, 3158 (1994).

[7] J. Reichel, F. Bardou, M. Ben Dahan, E. Peik, S. Rand, C. Salomon, and C. Cohen-Tannoudji, Phys. Rev. Lett. **75**, 4575 (1995).

[8] N. R. Newbury, C. J. Myatt, E. A. Cornell, and C. E. Wieman, Phys. Rev. Lett. **74**, 2196 (1995).

[9] M. Naraschewski, H. Wallis, and A. Schenzle, Phys. Rev. A **54**, 677 (1996).

[10] M. A. Ol'shanii and V. G. Minogin, Opt. Commun. **89**, 393 (1992).

[11] M. A. Ol'shanii, Opt. Spectrosk. **76**, 196 (1994) [Opt. Spectrosc. **76**, 174 (1994)].

[12] C. Foot, H. Wu, E. Arimondo, and G. Morigi, J. Phys. (France) II **4**, 1913 (1994).

[13] F. Bardou, J. P. Bouchaud, O. Emile, A. Aspect, and C. Cohen-Tannoudji, Phys. Rev. Lett. **72**, 203 (1994).

[14] P. Horak and H. Ritsch, Phys. Rev. A **55**, 2176 (1997); P. Horak and H. Ritsch, J. Opt. Soc. Am. B (to be published).

[15] P. Marte, R. Dum, R. Taïeb, P. Zoller, M. S. Shahriar, and M. Prentiss, Phys. Rev. A **49**, 4826 (1994).

[16] H. Wu, E. Arimondo, and C. Foot, Quantum Semiclassic. Opt. **8**, 983 (1996).

[17] F. Sander, T. Devolder, T. Esslinger, and T. W. Hänsch, Phys. Rev. Lett. **78**, 4023 (1997).

[18] C. W. Gardiner, *Quantum Noise* (Springer-Verlag, Berlin, 1991).

[19] Each single Zeeman sublevel is an eigenstate of the optical potential operator. The light shift they undergo is given by its eigenvalues: $\hbar U|\langle F_e,m_e|1,\pi;F_g,m_g\rangle|^2$. It is easily verified that the squared Clebsch-Gordan coefficients which appear in this expression have the required property.

[20] The compensation scheme is worked out starting from the optical potential operation light shifting the Zeeman components of the $|\Psi_{\rm nc}\rangle$ state and using the $m$ dependences of the Clebsch-Gordan coefficients for transitions driven by $\sigma_+$- and $\sigma_-$-polarized light fields. We stress that contrary to the $\pi$-polarized case, the relation between the coefficients forming the noncoupled superposition is needed to get the required $m^2$ dependence of the light shift. A more formal demonstration of the $\sigma_+$-$\sigma_-$ compensation has been presented to us by M. A. Ol'shanii (private communication).

[21] T. Pellizzari and H. Ritsch, Europhys. Lett. **31**, 133 (1995).

[22] Y. Castin and J. Dalibard, Europhys. Lett. **14**, 761 (1991).

[23] R. Dum, P. Marte, T. Pellizzari, and P. Zoller, Phys. Rev. Lett. **73**, 2829 (1994).

[24] G. Nienhuis, P. van der Straten, and S.-Q. Shang, Phys. Rev. A **44**, 462 (1991).

[25] A. M. Steane, G. Hillenbrand, and C. J. Foot, J. Phys. B **25**, 4721 (1992).

[26] M. R. Doery, E. J. Vredenbregt, and T. Bergeman, Phys. Rev. A **51**, 4881 (1995).

[27] I. I. Sobel'man, *Introduction to the Theory of Atomic Spectra* (Pergamon Press, New York, 1972), Secs. 13 and 31.3.